

Original Paper

Calculations of Energy Shift of the Conduction Band-Edge in Doped and Compensated GaP

Tamio ENDO, Nobuhiko ITOH, Yasushi OKINO
Yoshinori SHIMADA, Hirohito WATANABE
and Koichi SUGIYAMA

(Department of Electrical and Electronic Engineering)

(Received September 16, 1989)

The energy shifts of the parabolic conduction band-edge at 77 and 300 K with doping the Te-donor in GaP were calculated in the nondegenerate system for the two cases ; unintentional and intentional compensations, using the two models proposed by Hwang and by Mahan. The total parabolic shift ΔE_H (ΔE_H), and the contributions of the exchange interaction $\Delta \mu_{ex}$ (ΔE_x) and of the Coulomb interaction $\Delta \mu_{cd}$ (ΔE_c) calculated by the Mahan's model (Hwang's model), increase with increasing donor concentration in the unintentional compensation system at 300 K. $\Delta \mu_{ex}$ is smaller than $\Delta \mu_{cd}$, whereas ΔE_x is much larger than ΔE_c , and $\Delta \mu_{ex} < \Delta E_x$ and $\Delta \mu_{cd} > \Delta E_c$. ΔE_H agrees well with the experimental parabolic shift $\Delta \delta$ while $\Delta E_H > \Delta \delta$. The energy gap narrowing ΔE_g calculated by the Mahan's model is much larger than the experimental energy gap narrowing ΔE_g . The results are interpreted as follows. $\Delta \mu_{ex}$ fairly estimates the exchange interaction since the Mahan's model takes account of the anisotropy and multivalley effects. $\Delta \mu_{cd}$ reasonably estimates the Coulomb interaction since the Mahan's model takes account of the self-consistent interaction energy of the electron-screened donor system. The overestimation of the hole-electron correlation energy may be a reason for $\Delta E_g > \Delta E_g$.

Key Words: calculation, parabolic energy-shift, exchange interaction, Coulomb interaction, donor doping, compensation, GaP

1. Introduction

Semiconductor physics has been developed by doping impurities into semiconductors, and it has expanded occasions of application of semiconductors to electronic engineerings. Typical applications of highly-doped semiconductors are lasers^{1), 2)}, light-emitting-diodes³⁾ and tunneling diodes^{4), 5)}. There is such an example that some characteristics of the high-temperature transistor made of GaP/AlGaP were improved by the heavy doping⁶⁾. An important problem arising from the heavy doping is a band edge modification^{7) - 12)}. It causes, for example, changes in wavelength of the laser radiated from GaAs depending on amounts of doping and compensation¹³⁾. This gap-narrowing effect is now even utilized in doping superlattices¹⁴⁾. Then it is necessary to elucidate the fundamental heavy-doping effects as well as to develop new materials for a creation of new semiconductor devices.

It is well known for the heavily-doped semiconductors that the gap between the parabolic conduction and valence bands shrinks, and further that deep band tails beneath the shifted parabolic bands extend into a forbidden gap^{15), 16)}. Wolff¹⁷⁾ has shown theoretically that an effect of electron-electron interaction is to screen donor-impurity fields which produces a nearly rigid downward shift of an unperturbed density-of-states of the conduction band. He has also shown that an effect of electron-donor Coulomb interactions is important further down in the conduction band, and produces some structure near the bottom of the band, i.e., a potential fluctuation. We hereafter distinguish these two modifications. We call the rigid band shift the "parabolic shift", and the structure at deep band edge caused by the potential fluctuation the "band tail". Such band edge modifications were investigated in detail for Ge by Pankove and Aigrain¹⁸⁾, for Si by Lee and Fossum¹⁹⁾ and for GaAs by Casey and Stern¹²⁾. However, there have been no detailed studies for other compound semiconductors such as GaP and InP. Kane⁸⁾, Halperin and Lax⁹⁾, and Casey and Stern¹²⁾ proposed models describing the density-of-states distributions at the band edges of the heavily-doped semiconductors, which interpret the changes of the optical absorption-edge spectra. But one cannot say that the models can completely interpret the experimental results for all semiconductors.

In this paper, we calculate the energy shift of the parabolic conduction band-edge in the donor(Te)-doped and compensated GaP. Two models are employed for the calculation of the parabolic shift with changing in the donor concentration, and the results are compared each other. The calculation is done for low and high temperatures for the two cases; the unintentional and intentional compensations. Knowledges concerning the effects of compensation and thermal activation of electrons on the parabolic shift are useful on considering its mechanism, and further they are utilized to predict amounts of the parabolic shift in various circumstances. The specific calculation for the substantial system of unintentionally compensated materials is significant because the parabolic shift shows complex behaviours which we cannot predict intuitively, and because we cannot calculate it using only the fundamental physical constants such as dielectric constant and effective mass. We need in the calculation the definite ways of changing of a donor level and a degree of compensation with changing in the donor concentration. We obtain these

informations by Hall experiment. Finally we make comparisons between the calculated and experimental results of the parabolic shift and energy gap narrowing with increasing the donor concentration, and make some discussions. In this paper, we write expressions in CGS unit. The calculation of the potential fluctuation and band tail in the same system will be reported in a following volume²⁰⁾.

2. Theoretical Models for the Parabolic Shift

2.1 Hwang's model²¹⁾

We consider an electron system in the conduction band in the impurity-doped n-type semiconductor crystals. The system of all electrons can be approximated by single electrons moving in a field of the screened impurity potentials provided that the whole conduction band is shifted downward by an amount equal to the exchange interaction energy ΔE_e and that a change in the effective mass m_e ($m_e = 0.35m_0$ for GaP) is negligible. The one electron Hamiltonian of the same system can be written as

$$H_1 = -\frac{\hbar^2 \nabla^2}{2m_e} + E_0 - \Delta E_e + V(x), \quad (1)$$

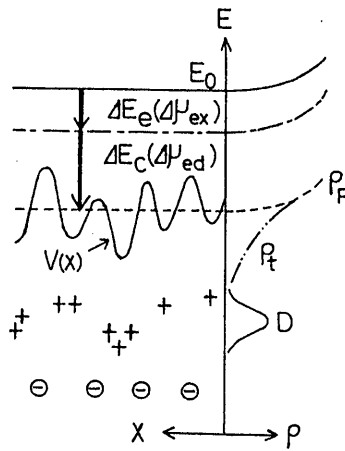


Fig.1 Schematic diagram showing the two contributions of ΔE_e (or $\Delta\mu_{ex}$) and ΔE_c (or $\Delta\mu_{ed}$) for the parabolic shift, and the spatial potential fluctuation $V(x)$ and the band tail of the conduction band-edge. The left hand side shows spatial coordinate (x) vs energy (E), and the right hand side density-of-states (ρ) vs E . The spatial and energy distributions of the donor ions are designated by +. The broadened donor states (D) are shown in the right hand side. The acceptor ions are designated by \ominus , the energies of them are not reflected.

where $\hbar = h/2\pi$ and h is the Planck constant, E_0 is the energy of the conduction band-edge in the nondoped crystal, and $V(x)$ is the screened potential of the randomly distributed impurities (Fig.1). Defining the average of $V(x)$ as ΔE_0 , such that the potential fluctuation about ΔE_0 is $V'(x) = V(x) - \Delta E_0$, we can then express H_1 as

$$H_1 = -\frac{\hbar^2 \nabla^2}{2m_0} + E_0 - \Delta E_0 - \Delta E_0 + V'(x) \quad (2)$$

This expression means that, as illustrated in Fig.1, the band edge energy is uniformly shifted downward by ΔE_0 due to the electron-electron exchange interaction and by ΔE_0 due to the dominant electron-donor ion Coulomb interaction in the case of donor-doped n-type system. The potential fluctuation $V'(x)$ is induced not only by the donor ions but also by the negatively charged acceptor ions in the compensated system. The magnitude of $V'(x)$ depends on the doping level of the donor and the degree of compensation. As shown in Fig.1, $V'(x)$ is pushed up in the repulsive region where the negative space charge exceeds while it is pulled down in the attractive region where the positive space charge exceeds. When $V'(x)$ is sufficiently large and attractive, a bound state localized in these regions is formed. The density-of-states (ρ_1) is called the band tail in such regions for energy $E < E_0 - \Delta E_0 - \Delta E_0$ (Fig.1). In the case of low level doping and low degree of compensation, we can neglect the potential fluctuation and band tail. We can neglect them also at high temperatures because the electrons have enough thermal energies to get over the potential hump and then completely screen the excess charge and smoothen out the potential fluctuation. In such the cases, we expect to find the parabolic density-of-states (ρ_0) for $E > E_0 - \Delta E_0 - \Delta E_0$ (Fig.1) and no density-of-states for $E < E_0 - \Delta E_0 - \Delta E_0$.

We deal with only the average parabolic shift in this work. We describe first the main theory of the parabolic shift proposed by Hwang^{2,1)}, and second by Mahan^{2,2)}. The both models are more accurate for the degenerate system at temperature $T=0$ K. It should be noted that if these models are employed for the nondegenerate system or the system at high temperatures, as we consider here, they give some uncertainty depending on the doping level and temperature. It is finally shown by comparing the calculated results with the experimental result that, in GaP system, the Hwang's model certainly overestimates the parabolic shift, however the Mahan's model gives better estimation of it. The potential fluctuation $V'(x)$ around the shifted average parabolic band edge and the band tail, will be reported in the following volume^{2,3)}.

The parabolic shift ΔE_0 caused by the exchange interaction is estimated by Wigner and Seitz^{2,3)} as

$$\Delta E_0 = \frac{4}{(4/9)^{1/3} \pi^{2/3} \eta} \frac{m_0 e^4}{2 \epsilon^2 \hbar^2} \quad (3)$$

where ϵ is the dielectric constant (10 for GaP) and e is an electron charge. η

is the ratio of the average electron spacing to the effective Bohr radius $a = \epsilon \hbar^2 / m_e e^2$ for electrons of concentration n_c in the conduction band. It is expressed

$$\eta = \frac{(3/4 \pi n_c)^{1/3}}{\epsilon \hbar^2 / m_e e^2} . \quad (4)$$

Then ΔE_c increases with increasing n_c as $n_c^{1/3}$. Equation (3) is accurate for $\eta < 1$ (degenerate case), whereas it gives some uncertainty for $\eta > 1$ (nondegenerate case). Then η gives the criterion for the application of eq.(3).

The parabolic shift ΔE_c caused by the Coulomb interaction is given also for $\eta < 1$ as

$$\Delta E_c = \frac{4 \pi e^2}{\epsilon} (N_D^+ - N_A^-) r_D^2 , \quad (5)$$

where N_D^+ is the positively ionized donor density, N_A^- is the negatively ionized acceptor density and r_D is a screening length. It can be expected straightforwardly from eq.(5) that the downward shift of ΔE_c increases with increasing N_D^+ owing to the attractive Coulomb interaction between the electrons in the conduction band and the donor ions, while ΔE_c decreases or the band edge is pushed up with increasing N_A^- owing to the repulsive Coulomb interaction between the electrons and the acceptor ions. Hwang used in his paper²¹⁾ trial values for the screening length r_D in eq.(5) in order to fit the calculated result to the experimental result. However, we simply try to use the Debye screening length for r_D in eq.(5) in this study. This is expressed

$$r_D = \frac{a}{2} \left(\frac{\pi}{3 a^3 n_c} \right)^{1/3} . \quad (6)$$

The Debye screening length is suitable for the degenerate and linear screening system. The total downward energy shift of the conduction band-edge is given by

$$\Delta E_H = \Delta E_c + \Delta E_e . \quad (7)$$

2.2 Mahan's model

Mahan's model²²⁾ takes account of an anisotropy, a multivalley effect and an electron distribution in the wave vector (k) space in a crystal. The downward parabolic shift ΔE_c caused by the exchange interaction which is denoted $\Delta \mu_{ex}$ in this model, is written as

$$\Delta \mu_{ex} = \frac{e^2 k_F}{\pi \epsilon} \Lambda . \quad (8)$$

In this equation, k_F is the Fermi wave vector given by

$$k_F = \left(\frac{3\pi^2 n_c}{M_c} \right)^{1/3}, \quad (9)$$

where M_c is the number of equivalent valleys of the bottom of conduction band ($M_c=6$ for GaP). The factor Λ in eq.(8) is the consequence of the anisotropic effective mass given by

$$\Lambda = (m_t/m_l)^{1/3} (\tan^{-1} \beta) / \beta, \quad (10)$$

$$\beta = [(m_l - m_t)/m_t]^{1/2}, \quad (11)$$

where m_t and m_l are the transverse and longitudinal effective masses. We use $m_t=0.2m_0$ and $m_l=1.7m_0$ in the calculation for GaP.

The downward parabolic shift ΔE_c caused by the Coulomb interaction which is denoted $\Delta \mu_{\infty}$ in this model, is written as

$$\Delta \mu_{\infty} = \frac{e^2 k_s}{8\epsilon}, \quad (12)$$

where k_s is the screening wave vector given by

$$k_s = \left(\frac{6\pi e^2 n_c}{\epsilon E_F} \right)^{1/2}. \quad (13)$$

In this equation, E_F is the Fermi energy given by

$$E_F = \frac{\hbar^2 k_F^2}{2m_d}, \quad (14)$$

where m_d is the density-of-states effective mass taking the anisotropy into account. This is given by

$$m_d = (m_t^2 m_l)^{1/3}, \quad (15)$$

for the single valley. We use $m_d=0.4m_0$ for GaP. One should mind that the definition of k_F and then the definitions of E_F and k_s are somewhat vague for the nondegenerate system. The total downward energy shift of the parabolic conduction band-edge is given by

$$\Delta E_n = \Delta \mu_{\infty} + \Delta \mu_{\infty}. \quad (16)$$

We would refer to the change in the energy gap in this model. In order to calculate it, we must deal with the parabolic shift of the valence band-edge in this system. If the hole in the valence band is considered to be the fixed charge, the effect of the hole-donor interaction and that of the hole-electron interaction on the shift of the valence band-edge improperly cancel out each other. Instead of this way of thinking, we should properly consider the hole

self-energy and the hole interaction energy with the combined donor-electron system, i.e., with the screened donor system. The hole is able to rearrange the electron density in its vicinity in order to lower the energy of the hole. This results in one of the hole self-energy called the hole-electron correlation energy. It is written as

$$\Sigma_{ho} = \frac{2e^2(0.8)}{\pi \epsilon} \left(\frac{m_h \omega_p}{2\hbar} \right)^{1/2}, \quad (17)$$

where m_h is the effective mass of holes ($m_h=0.653m_0$ for GaP). The plasma frequency is given by

$$\omega_p = (4\pi e^2 n_0 / m_d)^{1/2}. \quad (18)$$

Σ_{ho} is the upward energy shift of the valence band-edge. The other hole self-energy owing to the hole-screened donor interaction is approximately given by

$$\Sigma_{hd} \sim e^2 k_s / 8\epsilon. \quad (19)$$

This is the downward energy shift of the valence band-edge due to the repulsive Coulomb interaction. The hole-hole interaction effect can be neglected because the hole density is negligibly small. Then the total upward energy shift of the valence band-edge is given by

$$\Sigma_h = \Sigma_{ho} - \Sigma_{hd}. \quad (20)$$

The energy gap narrowing ΔE_g from the gap of the nondoped system is thus given by

$$\begin{aligned} \Delta E_g &= \Delta E_c + \Sigma_h \\ &= \Delta \mu_{ex} + \Delta \mu_{ed} + \Sigma_{ho} - \Sigma_{hd} \\ &= \Delta \mu_{ex} + \Sigma_{ho}. \end{aligned} \quad (21)$$

In this equation, the terms of $\Delta \mu_{ed}$ and Σ_{hd} cancel out each other. Then there remain in the expression only two terms; the electron-electron exchange interaction $\Delta \mu_{ex}$ corresponding to the downward shift of the conduction band-edge and the hole-electron correlation Σ_{ho} corresponding to the upward shift of the valence band-edge. In this model, we neglect the variational terms arising from the nonuniform distributions of the electrons and holes since its effect is small.

3. Calculation of Carrier Concentration

In general, as donor impurities are doped into semiconductors, it is unavoidable that acceptor-type impurities and defects are unintentionally introduced. We call it the unintentional compensation. The concentration of these acceptors N_a depends on the donor concentration N_d . In addition, the effective donor level ΔE_d from the conduction band-edge decreases with

increasing N_D due to a broadening of the donor level. In order to calculate specifically the parabolic shift on doping in GaP, we must determine the definite relationships between N_a and N_D , and ΔE_D and N_D . The Hall Measurement was made at various temperatures (T) between 77 and 300 K on various GaP samples doped with Te-donor for this purpose. Temperature dependences of the carrier concentration (n_c) were obtained from this experiment for the samples with different doping levels. We determine the relationships among N_D , N_a and ΔE_D by fitting the calculated n_c - T curves to the experimental plots of n_c - T . The method of calculation of n_c - T is described below.

The charge neutrality condition of the compensated semiconductor is expressed

$$n_c + N_a^- = N_D^+ = N_D - n_D, \quad (22)$$

where n_D is the neutral donor concentration. We assume here that $N_a = N_a^-$ since the energy levels of the compensating acceptors are thought to be very deep in the forbidden gap. n_c in eq.(22) is expressed on the Fermi statistics as

$$n_c = N_c f(E_c), \quad (23)$$

where N_c is the effective density-of-states of the conduction band located at energy $E = E_c$, and f is the Fermi distribution function. N_c is given by

$$N_c = 2 \left(\frac{2\pi m_d k_B T}{h^2} \right)^{3/2}, \quad (24)$$

where k_B is the Boltzmann constant. f is expressed as functions of E and T by

$$f(E) = \frac{1}{1 + \exp \{ (E - E_F) / k_B T \}}. \quad (25)$$

n_c in eq.(22) is expressed

$$n_D = \frac{N_D}{1 + \frac{1}{2} \exp \left(-\frac{E_D - E_F}{k_B T} \right)}, \quad (26)$$

where E_D is the donor level. Using E_c and E_D , the depth of the donor level ΔE_D is defined as $\Delta E_D = E_c - E_D$. We can calculate n_c as a function of T with a computer using eqs.(22)~(26) when the values of N_D , N_a and ΔE_D are given. It should be noted that we also calculated n_c by an integration method using the parabolic density-of-states distribution function instead of using N_c in eq.(23). It was, however, confirmed that this result is almost the same with the result obtained by using eq.(23). In the both calculations, we ignored the consequence of the band tail.

4. Results of the Calculated n_c vs N_D and the Criterion η

4.1 Relationships among N_D , N_A and ΔE_D

We calculated n_c as a function of T using eqs.(22)~(26) by giving trial values for N_D , N_A and ΔE_D . Thus obtained n_c - T curves were fitted to the experimental plots of n_c - T by making N_D , N_A and ΔE_D as adjustable parameters for the various samples. From this procedure, we could obtain several sets of values for N_D , N_A and ΔE_D , and could determine the definite relationships among them. They are expressed as

$$N_A = (41900 + 0.3140 \times N_D^{1/3})^3 \quad [\text{cm}^{-3}], \quad (27)$$

$$\Delta E_D = 102 - 1.35 \times 10^{-5} \times N_D^{1/3} \quad [\text{meV}]. \quad (28)$$

N_A increases with increasing N_D , and the magnitude of N_A is smaller than that of N_D by an order or more. This is the unintentional compensation in the substantial GaP samples. ΔE_D decreases with increasing N_D as $N_D^{1/3}$, and goes to zero at $N_D = 4.31 \times 10^{20} \text{ cm}^{-3}$. This indicates that the Te-donor state merges in the conduction band-edge, then the system becomes degenerate for $N_D > 4.31 \times 10^{20} \text{ cm}^{-3}$. This critical value is much higher than that of Si and GaAs, since the donor level is quite deeper in GaP than in Si and GaAs as mentioned later.

4.2 n_c as a function of N_D

We can determine the relation between n_c and N_D in the substantial system of the Te-doped GaP by means of the statistical calculations using eqs.(22)~(26), and further using the definite relationships between N_A and N_D , and ΔE_D and N_D expressed in eqs.(27) and (28). Figure 2 shows the calculated results of n_c as a function of N_D in the unintentional compensation system. In this figure, the upper abscissa is scaled by N_A using eq.(27). We will calculate in this work various parameters concerning the parabolic shift for low (77 K) and high (300 K) temperature cases. So that, n_c is shown at 77 and 300 K. n_c at 300 K increases with increasing N_D . The value of n_c , however, is only 80~20 % of that of N_D in the range of $10^{17} \sim 10^{19} \text{ cm}^{-3}$ of N_D . The rests of electrons are captured in the acceptor centers or remain unionized in the donor levels. When temperature is lowered to 77 K, n_c is drastically decreased by about four orders of magnitude. This implies that the system is not degenerate even at $N_D = 1 \times 10^{19} \text{ cm}^{-3}$ as mentioned above. The majority of electrons are bound to the neutral donors.

4.3 The criterion η

We examined the criterion η defined by eq.(4). We used n_c shown in Fig.2 to calculate η . η is shown in Fig.3 as a function of N_D together with $N_A a^3$. $N_D a^3$ is the volume fraction of the region where wave function of the donors is spreading provided that a spread of a donor wave function has the effective Bohr radius a (15 Å for GaP). We can judge from this figure that the system is

nondegenerate for $N_D < 2.5 \times 10^{20} \text{ cm}^{-3}$ which corresponds to $\eta > 1$. This result is almost the same with that estimated from $\Delta E_D \rightarrow 0$. $N_D a^3$ approaches unity at $N_D = 2.9 \times 10^{20} \text{ cm}^{-3}$, which also implies that the transition from the nondegenerate to the degenerate states occurs at this concentration. The critical concentrations of $N_D = 2.5 \sim 4.3 \times 10^{20} \text{ cm}^{-3}$ obtained by the various estimations are considerably higher in GaP than in Si and GaAs as mentioned above in terms of ΔE_D . The fundamental reasons are the much larger effective mass m_0 and the smaller dielectric constant ϵ for GaP. They lead to the smaller effective Bohr radius a and to the deeper donor level ΔE_D as can be deduced from the hydrogen model of the impurity state. We hereafter deal with the nondegenerate region of $N_D < 10^{19} \text{ cm}^{-3}$, then the calculated results are not so accurate for both the Hwang's model and the Mahan's model.

5. Results of the Parabolic Shift

5.1 Hwang's model

We treat the unintentional compensation alone in the Hwang's model. At the first, we should mention the Debye screening length r_D expressed by eq.(6). The calculated r_D is shown in Fig.4 at 77 and 300 K. r_D decreases with increasing N_D , which indicates that the screening effect becomes stronger, since r_D decreases as $(1/n_c)^{1/6}$ and n_c increases with increasing N_D as shown in Fig.2. r_D at 77 K is much larger than that at 300 K, which indicates that the screening effect is weaker at 77 K, since n_c at 77 K is much smaller than that at 300 K as shown in Fig.2.

The calculated results of ΔE_c , ΔE_v and the total parabolic shift $\Delta E_H =$

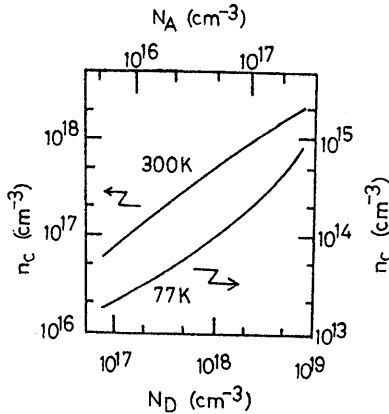


Fig.2 The calculated curves of n_c as a function of N_D for $T = 77$ and 300 K in the unintentional compensation system of Te-doped GaP. The upper abscissa is scaled by N_A using eq.(27).

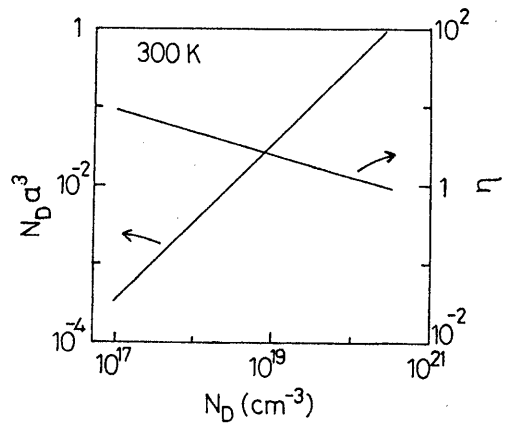


Fig.3 η and $N_D a^3$ as a function of N_D .

$\Delta E_v + \Delta E_c$ are shown in Fig.5 as a function of N_D at 300 K. ΔE_v was calculated by eqs.(3) and (4), and ΔE_c by eqs.(5) and (6). These quantities increase with increasing N_D . The increase in ΔE_v can be easily understood by the fact that n_i increases and then η decreases in eqs.(4) and (3) respectively. It can be suggested by the increase in ΔE_c that N_D^+ in eq.(5) increases overcoming the increase in N_A^- caused by the unintentional compensation, and further that the rate of decrease in r_D^{-2} is much smaller than that of increase in N_D^+ in eq.(5)

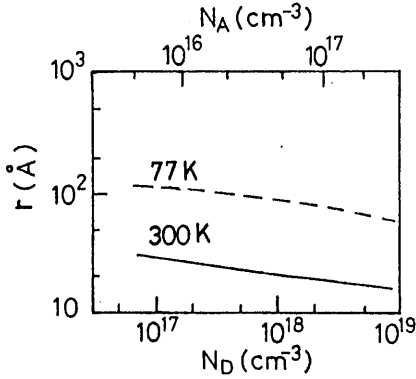


Fig.4 r_D as a function of N_D .

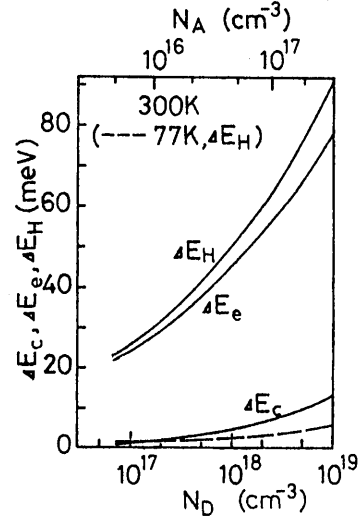


Fig.5 ΔE_v , ΔE_c and ΔE_H as a function of N_D .

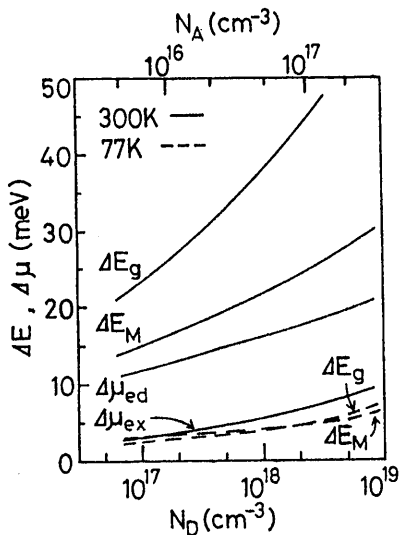


Fig.6 $\Delta \mu_{ex}$, $\Delta \mu_{ed}$, ΔE_M and ΔE_g as a function of N_D .

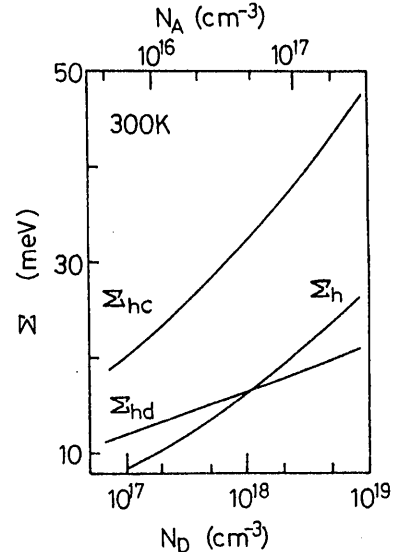


Fig.7 Σ_{hc} , Σ_{hd} and Σ_h as a function of N_D .

since r_D^2 decreases as no more than $(1/n_c)^{1/3}$ with increasing n_c in eq.(6). The latter indicates that the increase in the screening effect on the donor ions is weaker than the increase in the Coulomb effect on the parabolic shift due to the increase in N_D^+ . ΔE_H at 77 K is also shown in Fig.5, it is much smaller than ΔE_H at 300 K. This can be easily understood for the contribution of ΔE_c from the result that n_c at 77 K is much smaller than n_c at 300 K as shown in Fig.2. It can be suggested for the contributions of ΔE_c that ΔE_c decreases with decreasing T since N_D^+ decreases drastically in eq.(5) while r_D^2 increases not so much as shown in Fig.4. This indicates that the contribution of the screening effect is again weaker than that of the Coulomb effect in the case of temperature change. The decrease in N_D^+ with decreasing T equals the decrease in n_c shown in Fig.2, which can be recognized from eq.(22). Under this condition, n_D is to increase complementally.

5.2 Mahan's model

5.2.1 Unintentional compensation

The calculated results of $\Delta \mu_{ex}$, $\Delta \mu_{ed}$ and the total parabolic shift $\Delta E_H = \Delta \mu_{ex} + \Delta \mu_{ed}$ are shown in Fig.6 as a function of N_D at 300 K for the unintentional compensation system. These quantities increase with increasing N_D . $\Delta \mu_{ex}$ in eq.(8) increases as $n_c^{1/3}$ through k_F in eq.(9). $\Delta \mu_{ed}$ in eq.(12) increases as $n_c^{1/6}$ through k_s , E_F and k_F in eqs.(13),(14) and (9). ΔE_H at 77 K is also shown in Fig.6. It is much smaller than ΔE_H at 300 K. The reason is the much smaller n_c at 77 K for the both contributions of $\Delta \mu_{ex}$ and $\Delta \mu_{ed}$.

Before going into the energy gap narrowing, we should show the results for the valence band-edge. Figure 7 shows the calculated results of the upward shift Σ_{hc} , the downward shift Σ_{hd} and the total upward shift $\Sigma_h = \Sigma_{hc} - \Sigma_{hd}$ as a function of N_D at 300 K. Σ_{hc} in eq.(17) increases as $n_c^{1/2}$ through ω_p in eq.(18). Σ_{hd} in eq.(19) increases as $n_c^{1/6}$ with the same as $\Delta \mu_{ed}$ in eq.(12). The magnitude of Σ_{hc} is larger than that of Σ_{hd} , which results in the net upward shift Σ_h of the valence band-edge.

The energy gap narrowing $\Delta E_g = \Delta \mu_{ex} + \Sigma_{hc}$ is shown in Fig.6 as a function of N_D at 300 K. It increases with increasing N_D . The contributions of the downward shifts of $\Delta \mu_{ed}$ in Fig.6 and of Σ_{hd} in Fig.7 cancel out each other. Because of this cancelation, the magnitude of ΔE_g is restricted from

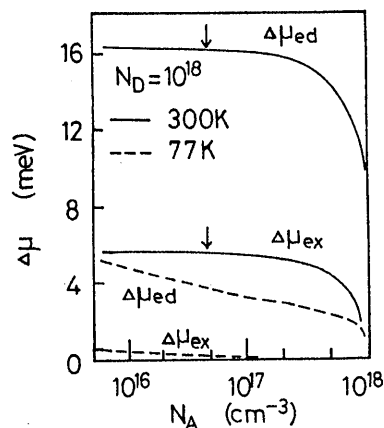


Fig.8 $\Delta \mu_{ex}$ and $\Delta \mu_{ed}$ as a function of N_A for $N_D = 1 \times 10^{18} \text{ cm}^{-3}$ in the intentional compensation system. The arrows indicate the unintentional compensation points.

being large. ΔE_c at 77 K is also shown in Fig.6. It is much smaller than ΔE_c at 300 K. The reasons are smaller $\Delta \mu_{ex}$ and Σn_c depending on the much smaller n_c at 77 K.

5.2.2 Intentional compensation

In the neighbouring region of the interface in p-n junctions such as laser diodes and LED's, the compensation of donors and acceptors with each other is more or less inevitable. Then it is useful to investigate the effects of the various degrees of compensation on the parabolic shift. We, therefore, calculate the parabolic shifts with increasing degree of compensation, i.e., with increasing N_A under constant N_D at 77 and 300 K. The two contributions of $\Delta \mu_{ex}$ and $\Delta \mu_{ed}$ are shown in Fig.8 as a function of N_A in a case of $N_D=1 \times 10^{18} \text{ cm}^{-3}$. In the such calculations, N_A^- in eq.(22) was arbitrarily increased. $\Delta \mu_{ex}$ and $\Delta \mu_{ed}$ decrease with increasing N_A at 77 and 300 K because of the decrease in n_c , however the decreasing manners are different for the two temperatures. $\Delta \mu_{ex}$ and $\Delta \mu_{ed}$ at 300 K decrease little until N_A exceeds $1 \times 10^{17} \text{ cm}^{-3}$ (the compensation ratio is $N_A/N_D=0.1$ at this concentration), then begin to decrease remarkably, and finally they decrease drastically as N_A approaches $1 \times 10^{19} \text{ cm}^{-3}$. The arrows indicate the points in the case of the unintentional compensation. Therefore it can be judged from these curves that the unintentional compensation affects little on $\Delta \mu_{ex}$ and $\Delta \mu_{ed}$ at 300 K for $N_D=1 \times 10^{18} \text{ cm}^{-3}$. On the other hand, $\Delta \mu_{ex}$ and $\Delta \mu_{ed}$ at 77 K decrease considerably over a wide range of N_A .

The total parabolic shifts ΔE_M at 300 and 77 K are shown as a function of N_A in Figs.9 (a) and (b) respectively for the constant N_D of 1×10^{17} , 1×10^{18} and $1 \times 10^{19} \text{ cm}^{-3}$. In these figures, the arrows indicate the points in the cases of the unintentional compensation. ΔE_M at 300 K for each N_D shows little

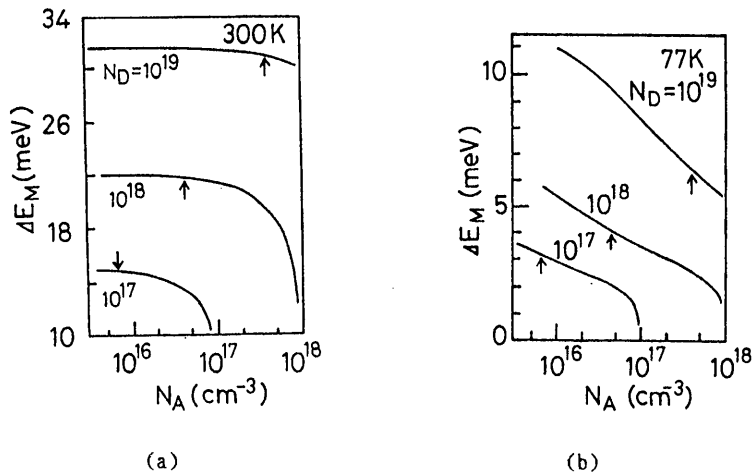


Fig.9 ΔE_M as a function of N_A for $N_D=1 \times 10^{17}$, 1×10^{18} and $1 \times 10^{19} \text{ cm}^{-3}$ in the intentional compensation system at (a) 300 K and (b) 77 K. The arrows indicate the unintentional compensation points.

decrease with increasing N_A until N_A/N_D reaches 0.1, and then shows drastic decrease. Thus the effect of the unintentional compensation on ΔE_H is again very small at 300 K. On the other hand, ΔE_H at 77 K for each N_D shows serious decrease over the wide range of N_A , then it can be judged that the effect of the unintentional compensation on ΔE_H is much larger at 77 K. It is clearly observed from Fig.9(b) that ΔE_H for $N_D=1 \times 10^{17} \text{ cm}^{-3}$ approaches zero as N_A reaches $1 \times 10^{17} \text{ cm}^{-3}$. This is explained as that n_c goes to zero for the full compensation of $N_A/N_D=1$.

5.2.3 Comparison of the calculated and experimental results

We compare first the calculated result of ΔE_H with the experimental result of the parabolic shift at 300 K. We have investigated the change in the splitting energy δ between the conduction band first minimum X_1 and the second minimum X_3 as a function of N_D in the Te-doped GaP by means of the optical absorption measurement at 300 K²⁴⁾. The experimentally obtained δ is plotted in Fig.10 as a function of N_D for the unintentional compensation system. This change in δ is thought to be caused by the average downward shift of the lower conduction band X_1 on doping, since it can be thought that the upper conduction band X_3 is fixed in energy on doping²⁴⁾. If δ at a sufficiently low N_D of $1 \times 10^{15} \text{ cm}^{-3}$ is taken as the splitting energy δ_0 for the nondoped system, $\Delta \delta = \delta - \delta_0$ is thought to correspond to the amount of the average parabolic shift of the conduction band-edge on doping from the pure material. The value of δ_0 was obtained from extrapolating a dashed line in Fig.10 which shows well an

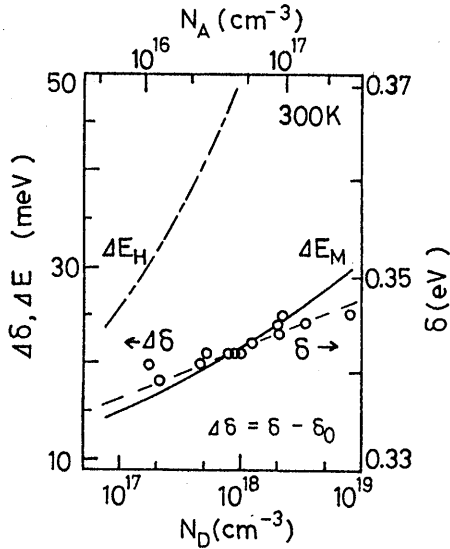


Fig.10 ΔE_H , ΔE_M and the experimental plot of $\Delta \delta$ as a function of N_D in the unintentional compensation system. The right ordinate is scaled by δ .

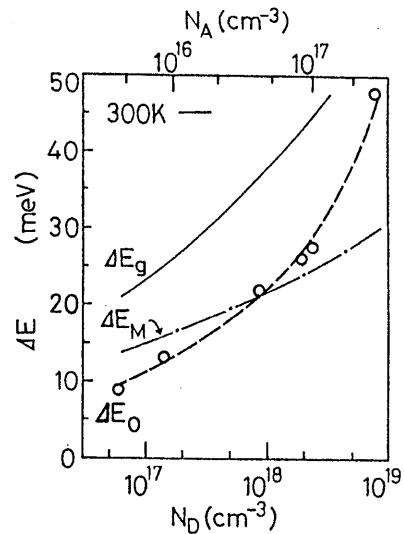


Fig.11 ΔE_G , ΔE_M and the experimental plot of ΔE_0 as a function of N_D in the unintentional compensation system.

experimental dependence of δ on N_D , because we could not directly obtain δ at such low N_D by means of the optical absorption measurement due to the very low carrier concentration. $\Delta\delta$ is scaled on the left ordinate for the same plot of δ in Fig.10. $\Delta\delta$ increases with increasing N_D . The calculated result of ΔE_H at 300 K is shown in Fig.10 as a function of N_D by a solid curve. ΔE_H agrees quite well with $\Delta\delta$ especially around $N_D=1\times 10^{18}$ cm⁻³, and ΔE_H slightly deviates from $\Delta\delta$ around $N_D=1\times 10^{17}$ and 1×10^{19} cm⁻³.

A curve of ΔE_H-N_D is also shown in Fig.10 by a dot-dashed curve. ΔE_H is considerably larger than ΔE_C and then than the experimental plot of $\Delta\delta$.

We compare second the calculated result of ΔE_C with the experimental result of the energy gap narrowing ΔE_0 . The calculated ΔE_C and the experimental ΔE_0 are shown in Fig.11 as a function of N_D at 300 K. The plot of the experimental ΔE_0 has been obtained by the measurement of the fundamental absorption edge for the Te-doped GaP with different N_D 's. The calculated ΔE_C is larger than the experimental ΔE_0 by 10-15 meV. The calculated shift ΔE_H of the conduction band alone is also shown in Fig.11 for a reference. The experimental ΔE_0 is closer to ΔE_H rather than ΔE_C in the middle range of N_D .

6. Discussion

The detailed arguments were already done in sections 4 and 5. We discuss here the comparative and general arguments for the results of the parabolic shift and the energy gap narrowing.

The contribution of the exchange interaction ΔE_x is much larger than that of the Coulomb interaction ΔE_c in the Hwang's model at 300 K (Fig.5). On the contrary, the contribution of the exchange interaction $\Delta\mu_{ex}$ is smaller than that of the Coulomb interaction $\Delta\mu_{ec}$ in the Mahan's model at 300 K (Fig.6). In addition, the value of ΔE_x is notably higher among the values of these parameters. It can be judged that ΔE_x overestimates the exchange interaction as supported by the comparison of the total parabolic shift ΔE_H with the experimental $\Delta\delta$ (Fig.10). In contrast with the Hwang's model, the Mahan's model takes account of the anisotropy and multivalley effects, and the electron distribution in the k-space in the conduction band. So that, it can be suggested that $\Delta\mu_{ex}$, which is much smaller than ΔE_x , reasonably estimates the exchange interaction. The reason for the very small Coulomb interaction ΔE_c is the small Debye screening length r_D which we used in the Hwang's model. That is, the screening effect is overestimated. It is judged that the application of the Debye screening length, which is essentially suitable to the degenerate system, is unreasonable since it is too small in the present nondegenerate system. The screening length calculated by the nonlinear screening theory is certainly larger than r_D by an order of magnitude. If this nonlinear screening length is used, the calculation of ΔE_c is somewhat improved. We shall not mention it in this paper. In contrast with the Hwang's model, the Mahan's model takes account of the self-consistent interaction energy of the electron-screened donor system for the Coulomb interaction $\Delta\mu_{ec}$. This model uses the same electron wave function for the electron in the conduction band and for the electron as the screening charge. That is, all of the conduction electron

charge is located as screening charge, and the overlap of adjacent screening units is ignored. Therefore, the screening effect is reasonably taken into account for $\Delta \mu_{\text{sc}}$. $\Delta \mu_{\text{sc}}$, which is larger than ΔE_0 , must give the better estimation for the Coulomb interaction. The incorporation of the multivalley effect is also one of the causes for the better estimation of $\Delta \mu_{\text{sc}}$. The value of $M_0=6$ in eq.(9) leads to the larger $\Delta \mu_{\text{sc}}$ than $\Delta \mu_{\text{sc}}$ for $M_0=1$.

Because of the interpretations mentioned above, the parabolic shift ΔE_H calculated by the Mahan's model agrees well with the experimentally obtained parabolic shift $\Delta \delta$ at 300 K as shown in Fig.10. The parabolic shift ΔE_H calculated by the Hwang's model is remarkably larger than $\Delta \delta$, which is caused by the overestimation of ΔE_0 .

Strictly speaking, the Mahan's model is applicable to the degenerate system at $T=0$. This implies that it is not necessary in this model to take account of the neutral donor state in which an electron is bound to a donor atom for the Coulomb interaction of the electron-screened donor system. However, in the present study, the neutral donor must be taken into account. Though, it is a difficult problem to clarify what effect the neutral donor has on the parabolic shift. It will be necessary in the future to take this effect into account in the nondegenerate system.

The energy gap narrowing ΔE_0 calculated by the Mahan's model is larger than the experimental plot of ΔE_0 as shown in Fig.11. This difference may arise from the overestimation of Σ_{sc} for the shift of the valence band-edge, because it is thought that $\Delta \mu_{\text{sc}}$ in the expression of $\Delta E_0 = \Delta \mu_{\text{sc}} + \Sigma_{\text{sc}}$ gives the good estimation for the shift of the conduction band-edge. This judgment is supported by the fact that $\Delta E_H (= \Delta \mu_{\text{sc}} + \Delta \mu_{\text{sc}})$ agrees well with the experimental $\Delta \delta$ (Fig.10). The experimental ΔE_0 is closer to the calculated ΔE_H rather than the calculated ΔE_0 . This might indicate that the energy gap narrowing is predominantly caused by the shift of the conduction band-edge in the present system of the Te-doped and unintentionally compensated GaP. The reasons for the smaller ΔE_0 (Fig.11) than $\Delta \delta$ (Fig.10) in the region of lower N_D may be the difference of the definitions of ΔE_0 and $\Delta \delta$, and the experimental error.

7. Summary

The parabolic shifts of the conduction band-edge at 77 and 300 K were calculated for the donor(Te)-doped and the unintentionally and intentionally compensated GaP in the nondegenerate system employing the Hwang's model and the Mahan's model. The contributions of the exchange interaction and the Coulomb interaction, and the total parabolic shift increase with increasing donor concentration in the unintentional compensation system. Hwang's model gives the overestimation of the exchange interaction, and gives the underestimation of the Coulomb interaction because the small Debye screening length was used. As a result, the total parabolic shift calculated by this model is much larger than the experimental parabolic shift.

Since the Mahan's model takes account of the anisotropy and multivalley effects, and the electron distribution in the k-space, it gives a good estimation of the exchange interaction. This model takes account of the self-

consistent interaction energy of the electron-screened donor system, so that it gives a good estimation of the Coulomb interaction. As a result, the total parabolic shift calculated by this model agrees well with the experimental parabolic shift especially around $N_D = 1 \times 10^{18} \text{ cm}^{-3}$. The energy gap narrowing calculated by this model is much larger than the experimental energy gap narrowing. The reason may be the overestimation of the hole-electron correlation energy, namely, the overestimation of the shift of the valence band-edge. Then there is still some room for improvement to apply the Mahan's model to the present GaP system.

The effects of the intentional compensation were investigated at 77 and 300 K on the contributions of the exchange interaction and the Coulomb interaction, and on the total parabolic shift calculated by the Mahan's model. The parabolic shift decreases little with increasing degree of compensation until N_A/N_D reaches 0.1, and then decreases remarkably at 300 K. On the contrary, the parabolic shift considerably decreases with increasing degree of compensation in the entire region of it at 77 K. Therefore, the unintentional compensation affects little on the parabolic shift at 300 K while it seriously affects at 77 K.

In the present study, we ignored the effect of electron distribution in the higher part of the conduction band due to the thermal energy $k_B T$ especially at 300 K. We hope that the theory, which accurately treat the nondegenerate system and the thermal effect, will be advanced.

Acknowledgements

The authors wish to express their thanks to Messrs. A. Nakanishi and K. Miyata for their help with the part of Hall experiment, and Messrs. M. Matsuyama and H. Miyake for preparation of the manuscript.

References

- 1) R. Hall: IEEE Trans. Electron Devices, ED-23, 700 (1976).
- 2) G. C. Dousmanis, H. Nelson and D. L. Staebler: Appl. Phys. Lett., 5, 174 (1964).
- 3) J. I. Pankove: J. Appl. Phys., 35, 1890 (1964).
- 4) L. Esaki: Phys. Rev., 109, 603 (1958).
- 5) L. Esaki and Y. Miyahara: Solid-State Electron., 1, 13 (1960).
- 6) T. E. Zipperian and L. R. Dawson: J. Appl. Phys., 54, 6019 (1983).
- 7) V. L. Bonch-Bruевич: Proc. Int. Conf. Physics of Semiconductors, Exeter (1962), p. 216.
- 8) E. O. Kane: Phys. Rev., 131, 79 (1963).
- 9) B. I. Halperin and M. Lax: Phys. Rev., 148, 722 (1966).
- 10) C. Haas: Phys. Rev., 125, 1965 (1962).
- 11) J. I. Pankove: Phys. Rev., 140, A2059 (1965).
- 12) H. C. Casey, Jr. and F. Stern: J. Appl. Phys., 47, 631 (1976).
- 13) P. D. Dapkus, N. Holonyak, Jr. and J. A. Rossi: J. Appl. Phys., 40, 3300 (1969).
- 14) K. Ploog, H. Jung, H. Künzel and P. Ruden: Proc. 14th Int. Conf. Solid

- State Devices, Tokyo (1982), Jpn. J. Appl. Phys., 22, Suppl. p.287 (1983).
- 15) F.Stern: Phys. Rev., 148, 186 (1966).
 - 16) M.B.Panish and H.C.Casey, Jr.: J. Phys. Chem. Solids, 28, 1673 (1967).
 - 17) P.A.Wolff: Phys. Rev., 126, 405 (1962).
 - 18) J.I.Pankove and P.Aigrain: Phys. Rev., 126, 956 (1962).
 - 19) D.S.Lee and J.G.Fossum: IEEE Trans. Electron Devices, ED-30, 626 (1983).
 - 20) T.Endo et al.: to be submitted to Res. Rep. Fac. Eng. Mie Univ., Vol.15 (1990).
 - 21) C.J.Hwang: Phys. Rev., B2, 4117 (1970).
 - 22) G.D.Mahan: J. Appl. Phys., 51, 2634 (1980).
 - 23) N.F.Mott and H.Jones: The Theory of Properties of Metals and Alloys, Dover, New York (1936) p.137.
 - 24) T.Endo, K.Sawa, Y.Hirosaki, S.Taniguchi and K.Sugiyama: Jpn. J. Appl. Phys., 26, 912 (1987).